Solid State Communications 282 (2018) 1–4

Contents lists available at ScienceDirect

Solid State Communications

journal homepage: www.elsevier.com/locate/ssc

Communication

Ferromagnetic Fe_2O_3 nanopatterns prepared using dip-pen lithography

Hyun Wook Shin, J.Y. Son*

Department of Applied Physics, Institute of Natural Sciences, College of Applied Science, Kyung Hee University, Suwon, 446-701, South Korea

ARTICLE INFO

Communicated by E.Y. Andrei

Keywords:
A. Ferromagnetic nanostructure
B. Dip-pen lithography
D. Magnetic properties
E. Magnetic force microscopy

ABSTRACT

Ferromagnetic Fe_2O_3 nanorings and nanorods were deposited on an SiO_2/Si substrate by dip-pen lithography using an iron nitrate $Fe(NO_3)_3{\cdot}9H_2O$ solution. Magnetic force microscopy (MFM) studies have shown that ferromagnetic Fe_2O_3 nanorings and nanorods have in-plane, oriented, and magnetic domain structures. In particular, nanorings have the vortex magnetization state, not the onion state. Their small-size fabrication and stable magnetic properties may suggest future applicability for next-generation magnetic media memory devices.

1. Introduction

In storage devices and in general, as electronic devices are aggressively scaled down to the nanoscale regime, the fabrication of nanostructured ferromagnetic devices is drawing considerable attention. To increase the memory density, an understanding of the fabrication of ferromagnetic nanostructures is necessary. Various ferromagnetic nanostructures of $BiFeO_3$, Ni, and Co have been synthesized or fabricated by sol-gel methods [1], nanotemplates [2], aqueous growth [3], and advanced nanolithography. Among these methods, the dip-pen nanolithography (DPN) technology based on scanning probe microscopy enables the production and handling of multiple ferroelectric and multiferroic nanostructures, such as $PbTiO_3$ and $BiFeO_3$ [4,5]. Because of the ability of atomic force microscopy (AFM) to control nanomaterials, the DPN technology has produced diverse nanopatterns using various materials, such as metals, semiconductors, proteins, cells, and even viruses [6,7]. The DPN method exploits the water meniscus formed between a slowly scanning AFM tip and a substrate to transfer the species on the tip to the substrate by diffusion. Previous research has employed a gold–thiol interaction to create robust patterns [8]. Recently, a wide variety of applications is available for investigating the various properties of nanostructures. Therefore, the DPN technology is expected a feasible solution for realizing position-controlled ferromagnetic nanostructures in magnetic storage media applications [9,10]. In particular, our previous studies have proved that the DPN technology enables the easy fabrication of ferroelectric and multiferroic nanodots with elaborately controlled lateral dimensions down to 20 nm, even at a specific position [4,11].

2. Experimental procedures

Fig. 1(a) and (b) show the schematics of the DPN process for preparing Fe_2O_3 nanostructures. SiO_2/Si substrates were used to form Fe_2O_3 nanostructures and thin films. To perform the DPN and thin film deposition processes of Fe_2O_3 nanostructures, iron nitrate $Fe(NO_3)_3{\cdot}9H_2O$ (Aldrich 98%) was employed as a precursor solution. An Si_3N_4 DPN tip with a diameter of approximately 10 nm was used at a speed of approximately 300 nm/s. The DPN nanostructures were kept at atmosphere for 24 h to gradually dry the solvent inside them. To crystallize the Fe_2O_3 nanostructures and thin films, they were annealed in a 100% oxygen gas environment at 400 °C for 1 h. The surface morphology and magnetic topography of the thin film were observed using an atomic force microscope (AFM, X-100, Park Systems) and a magnetic force microscope (MFM). Magnetic hysteresis loops of the Fe_2O_3 thin film were obtained using a superconducting quantum interference device magnetometer (Quantum Design.

3. Results and discussion

Fig. 2 shows an AFM image of a patterned Fe_2O_3 dot (a) and its diameter as a function of DPN time(b). From Fig. 2(a), it can be observed that the A pattern is almost 50 nm in diameter. This pattern size is smaller than that of previous Fe_3O_4 from the DPN process [12]. More interestingly, Fig. 2(b) shows the sizes of patterns with a clearly distinguished slope as a function of the DPN deposition time. Below 0.5 s, a high slope was observed, whereas above 2 s, a small slope was observed. At deposition times between 0.5 and 2 s, the slope exhibited a mixed regime. This can be explained by the kinetics of ink molecules transported from the AFM tip to the sample surface during the DPN

* Corresponding author.
E-mail address: jyson@khu.ac.kr (J.Y. Son).

https://doi.org/10.1016/j.ssc.2018.07.006
Received 28 October 2017; Received in revised form 23 June 2018; Accepted 16 July 2018
Available online 18 July 2018
0038-1098/

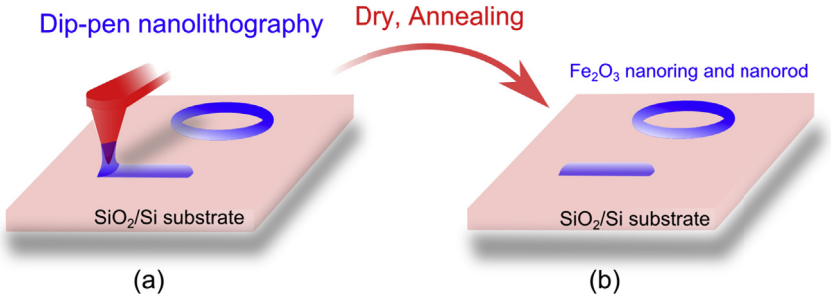

Fig. 1. Schematic drawings of the dip-pen nanolithography (DPN) process of ferromagnetic Fe_2O_3 nanostructures. (a) The formation of Fe_2O_3 nanorods and nanorings on the SiO_2/Si substrate using the DPN method. (b) The crystallization process of the Fe_2O_3 nanostructures by dry and annealing processes.

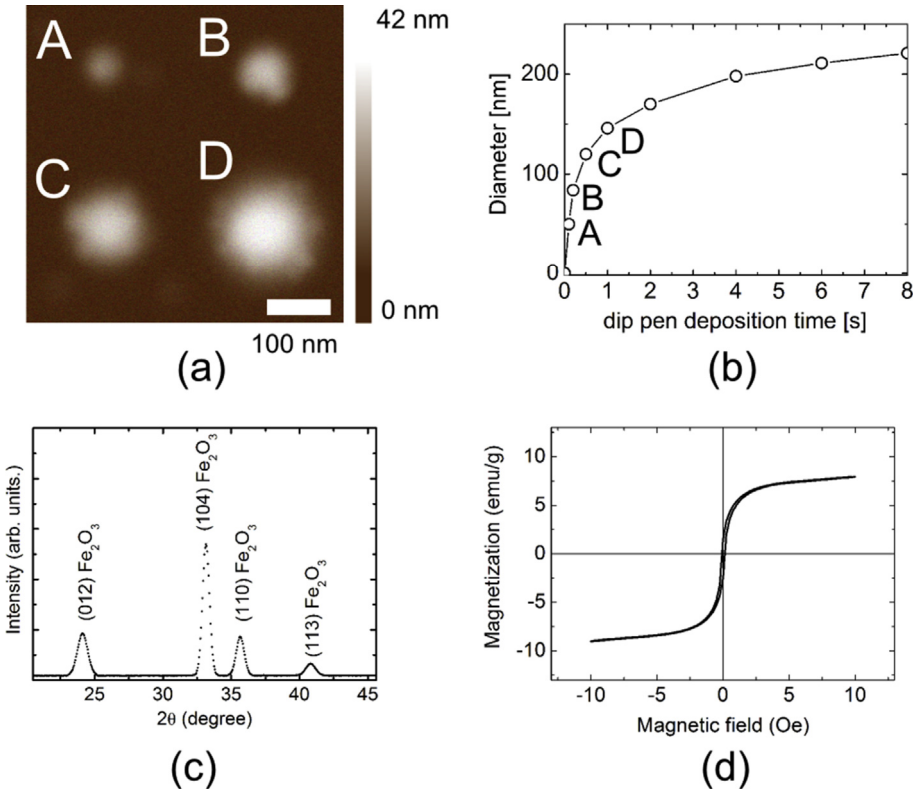

Fig. 2. (a) An atomic force microscopy (AFM) image of the Fe_2O_3 nanodotshaving various diameters by controlling the DPN time. (b) Diameters of the Fe_2O_3 nanodots as a function of DPN time. (c) XRD pattern of the Fe_2O_3 thin film deposited on the SiO2/Si substrate. (d) Ferromagnetic hysteresis loop of the Fe_2O_3 thin film.

process. The dot radius can be expressed by the following equations [13]:

$$R^2 = A\left[\beta_+\tau - \pi a^2\beta_-\int_0^\tau C_0(t)dt\right], \quad (1)$$

$$\beta_+ = \nu e^{-E_D/kT}, \quad \beta_- = \left(\frac{kT}{2\pi m}\right)^{1/2} e^{-E_A/kT}. \quad (2)$$

Here, R represents the dot radius, A represents the contact area between the tip and the meniscus, πa^2 is the average area per precursor molecule, and C_0 is the concentration of the precursor in the solution adjacent to the tip. In addition, E_D is the activation energy for ink detachment, E_A is the activation energy for attachment, k is Boltzmann's constant, T is the temperature, m is the mass of the precursor, and ν is the attempt frequency. For a short deposition time (τ), $C_0 \sim 0$ and the dot size $R^2 = A\tau$. In this regime, surface kinetics dominates the transfer process. In our case, the time seemed to be shorter than 0.5 s. For long deposition times, C_0 reaches an equilibrium concentration. Then, $R^2 = A\tau$; however, the slopes of these linear relationships are reduced. In this regime, the transfer process is controlled by diffusion and it can be observed after 2 s. We observed considerably similar dependencies in our experiments for dot fabrication. From these data, it is clear that the fabrication of Fe_2O_3 is successfully set up by the DPN method.

Since the Fe_2O_3 nanostructures of nanorods and nanorings were formed at the local areas on the SiO_2/Si substrates, it was hard to analyze the stoichiometries, structures, phases, and magnetic hysteresis loops of these nanostructures. Thus, we measured the XRD pattern of the Fe_2O_3 thin film deposited on SiO_2/Si substrate using the same precursor solution used for the formations of the Fe_2O_3 nanostructures as shown in Fig. 2(c). The Fe_2O_3 thin film as a polycrystalline thin film exhibits the (012), (104), (110), and (113) XRD peaks corresponding to the α-Fe_2O_3 phase (JCPDS, #330664). Thus, it is inferred that the Fe_2O_3 nanostructures have the α-Fe_2O_3 phase. Fig. 2(d) shows the magnetic hysteresis loop of the Fe_2O_3 thin film. The Fe_2O_3 thin film exhibited the canonical ferromagnetic hysteresis loop.

Fig. 3(a) shows an AFM image of an Fe_2O_3 nanorod prepared using the DPN method on a SiO_2/Si substrate. We successfully fabricated an approximately 50-nm-wide nanorod by controlling the DPN speed. Fig. 3(b) shows a vertical (upward polarized) MFM image of the nanorod. This image indicates that the laterally aligned Fe_2O_3 nanorod is characterized by a single magnetic domain with the magnetization parallel to the direction of its axis. To clarify the initial magnetization, a